Post-Mortem Analysis of Lithium-Ion Capacitors after Accelerated Aging Tests

Nagham El Ghossein, Ali Sari, Pascal Venet, Sylvie Genies, Philippe Azaïs

Version of Record: https://www.sciencedirect.com/science/article/pii/S2352152X20318739
Manuscript_2f52fb7108c179903971079c61d28533

Post-Mortem Analysis of Lithium-Ion Capacitors after Accelerated Aging Tests

Nagham El Ghossein[(1,2)], Ali Sari[(1)], Pascal Venet[(1)], Sylvie Genies[(3)], Philippe Azaïs[(3)]

[(1)] Univ Lyon, Université Claude Bernard Lyon 1, Ecole Centrale de Lyon, INSA Lyon, CNRS, Ampère, F-69100, Villeurbanne, France
[(2)] LabECAM, ECAM Lyon, Université de Lyon, 40 montée Saint-Barthélémy, F-69005 Lyon, France
[(3)] Univ. Grenoble Alpes, CEA, LITEN, DEHT, F-38000 Grenoble, France

Abstract

Lithium-ion Capacitors (LiCs) have recently emerged in the market of energy storage systems as a new technology having some of the advantages of Lithium-ion Batteries (LiBs) and Supercapacitors (SCs). As an important number of commercial LiCs combine the negative electrode of LiBs with the positive electrode of SCs, the lifetime of this new technology requires an effective analysis that can underlie degradation mechanisms related to each electrode. In order to evaluate the aging behavior of LiCs, calendar accelerated aging tests were applied to eighteen cells for twenty months in a previous study. Two temperatures, 60°C and 70°C, and three storage voltage values, 2.2 V, 3.0 V and 3.8 V were used to accelerate their aging. the The lifetime of LiCs was found to be particularly dependent on the storage voltage and the degradations of the cells were most pronounced at the highest temperature, 70°C. Therefore, in the current study, post-mortem analyses are applied to three cells that aged at different storage voltage values and 70°C. Considering the same aging mechanisms at high temperatures, only one high temperature was chosen. Two main aging mechanisms were observed: the pores blocking of activated carbon at the positive electrode and the loss of lithium ions from the negative electrode of pre-lithiated graphite. Elements responsible for these degradations were different at each voltage condition. Additional mechanisms were identified such as the degradation of the electrolyte and the decomposition of the positive current collector.

Keywords: Lithium-ion capacitor, Post-mortem analysis, Electrochemical impedance spectroscopy, Electrode degradation, Aging mechanisms, Electrochemical characterization

1. Introduction

Aging behavior of Energy Storage Systems (ESSs) depends on several factors related to their operational conditions, such as temperature, voltage range and current. The electrochemical properties of the cells degrade in different manners inducing the decrease of their electrical performances. For this reason, lifetime analysis of ESSs, prior to their integration in a specific application, can help in avoiding future failure, arranging predictive maintenance and reducing the total cost of the system.

In order to properly evaluate aging behavior of ESSs, accelerated aging tests are implemented and followed by post-mortem characterizations. Consequently, lifetime and aging mechanisms can be analyzed as well as possible enhancement of cells composition. Several research studies evaluated lifetime of Lithium-ion Batteries (LiBs) and Supercapacitors (SCs) [1]–[4].

However, Lithium-ion Capacitors (LiCs), which were recently developed for filling the gap between SC's low energy density and LiB's low power density [5], are still considered as a new technology with a limited number of studies on their lifetime. A considerable number of commercial LiCs are composed of a positive electrode of activated carbon, similar to the one used in SCs, and a negative electrode of pre-lithiated graphite that is usually employed in LiBs [6]. Concerning the aging of LiCs, multiple queries may arise, mainly related to the combination of degradation mechanisms of former ESSs in this new component.

The main aging mechanism in LiBs was found to be the growth of a passivation layer, known as Solid Electrolyte Interface (SEI), at the negative electrode when lithiated [7], [8]. Since LiCs possess a similar negative electrode, its aging may be a huge concern. This layer is originally formed during the first charge of the LiB. In fact, the electrolyte is decomposed at the surface of the graphite that is negatively charged due to its lack of thermodynamic stability. This happens at a potential range between 1.2 and 0.8 V with respect to the potential of Li/Li^+ and above the potential domain where the lithium insertion occurs (between 0.25 V and 0.01 V). Products of electrolyte decomposition, which can be organic or inorganic, form a passivation layer at the surface of the electrode. As a result, additional decomposition of the electrolyte is avoided while the transport of lithium ions is still assured during the cycling of the LiB [9]. The potential of the SEI formation cannot be assigned to a specific value, although 0.8 V vs. Li/Li^+ is the most commonly used one. This potential usually depends on the type of the electrode and the employed solvents [10]. At high temperatures, the SEI becomes unstable and several parasitic reactions might occur generating solid products such as Li_2CO_3 [11]. The properties of the modified passivation layer can significantly affect the performance of the battery. Its growth induces the decay of its capacity (i.e. reversible lithium ions) and the rise of its internal resistance [12]. Other aging mechanisms might affect the negative electrode of a LiB such as the exfoliation of the graphite due to the intercalation of the solvated lithium ions in its layers [9]. Moreover, at low potentials vs. Li/Li^+, metallic lithium may be deposited at the graphite electrode, especially at low temperatures. The persistent of dendritic lithium deposition can cause a short-circuit inside the battery cell which increases the risk of thermal runaway [13].

Since the positive electrode of LiCs is made of activated carbon, similarly to SCs, it is important to recall aging mechanisms of this electrode that were highlighted in SCs. In fact, after the chemical and thermal treatments of a carbon electrode, some functional groups may reside at its surface [14]. These treatments are used to produce pores in the electrode so its capacitance can be enhanced. At high temperature and voltage values, redox reactions are encouraged between these functional groups and electrolyte components. As a result, solid products may be deposited at the surface of activated carbon leading to the blocking of pores [2], [15]. Consequently, the total capacitance of the SC decreases. Moreover, gases may be generated inducing the increase of the pressure, which can make the packaging swell. These products can also be adsorbed at the surface of the activated carbon or even at the separator, which causes the decrease of the ionic conductivity. Therefore, the total resistance of the SC may significantly rise. The high pressure in the packaging of the SC may lead to electrodes cracking or the degradation of the current

collectors. This also extremely affects the series resistance of the SC. Post-mortem studies applied to a SC that had undergone calendar aging at high voltage and high temperature have shown that the local structure properties of the positive electrode change during aging [16]. Images obtained using field effect scanning electron microscopy before and after aging showed a noticeable change in the morphology of the electrode surface. In fact, larger crystals were formed and the surface of the electrode became less rough. In addition, the porosity of the positive electrode decreased, most likely because of pores blocking by the products of the electrolyte degradation.

Aging mechanisms of these electrodes may also appear in LiCs. However, the effect of the SEI growth on the aging of the negative electrode can most probably be reduced since the capacity of negative electrode is oversized with respect to the positive one. In fact, in [17], several sizing strategies were tested to find the optimal ratio between the masses of the positive electrode and the negative electrode. When the ratio was high (the mass of the positive electrode was larger than that of the negative electrode), the complete charge of the positive electrode was long enough for the negative electrode to operate over a large potential window. In fact, when the positive electrode has a higher mass than the negative electrode, the positive electrode can accept more charges which extends the time of charging. This results in an additional charge of the negative electrode whose potential varies accordingly. As a result, the potential of the negative electrode entered a region where the decomposition of the electrolyte started to occur. Therefore, a significant SEI layer was formed at its surface, which induced an increase of the series resistance of the LiC. On the other hand, a ratio lower than 1 (the mass of the negative electrode was larger than that of the positive electrode) induced a smaller charge transfer resistance. This configuration was based on a positive electrode with a smaller thickness than the previous one. The charge of the positive electrode was then faster, leading the negative electrode to operate over a smaller potential window. Consequently, the negative electrode intercalated a smaller amount of lithium ions in its structure and the growth of the SEI layer was less pronounced [17]. Moreover, the larger the negative electrode is, the higher the state of charge during storage can be, without reaching the regime that causes a strong degradation of the capacitance [18]. Even though few studies evaluated the aging of LiCs, the behaviors of the two electrodes of a LiC during a continuous cycling were analyzed in [19]. The tested LiC included a positive electrode of activated carbon and a pre-lithiated hard carbon negative electrode. The employed electrolyte was made of 1 mol/L $LiPF_6$ in a mixed solvent, EC/DMC/DEC (Ethylene Carbonate / DiMethyl Carbonate / Diethyl Carbonate). During cycling of the LiC, potential drift of electrodes was observed, followed by a decrease of the capacitance and an increase of the equivalent series resistance. The decay of the capacitance is attributed to the negative electrode of hard carbon. In fact, the increase of the internal resistance and the consumption of cyclable lithium ions are the causes of capacitance decrease during cycling. The resistances due to the SEI and the diffusion in the negative electrode increase progressively, leading to the increase of the polarization of the negative electrode and the reduction of its capacity. As a result, the negative electrode can no longer be fully charged (lithiated) and the capacitance of the LiC decreases. In addition, the consumption of lithium ions causes a positive drift of

the potential of the negative electrode and reduces the usable cathodic potential range. Therefore, raising the potential of the positive electrode accelerates the aging of LiCs [20]. Its potential should not usually exceed 4 V vs. Li/Li^+ [21]. Otherwise, the negative electrode degrades more rapidly. In fact, the higher the potential of the positive electrode is, the lower the capacity of the negative electrode becomes. This is attributed to a generation of lithium fluoride (LiF) when the positive activated carbon electrode is highly polarized [21]. The functional groups of the positive electrode can also participate in this product formation by providing H^+ ions.

The aging of commercial LiCs has not been well studied in the literature. Accelerated aging tests were applied in only one previous study [22]. As expected, it was proved that the higher the temperature is, the greater the degradation of LiCs becomes. For example, a calendar test at 60°C and 3.8 V resulted in a 10 % decrease of the capacitance after 5000 hours while another one at 0°C and 3.8 V caused a decrease of less than 2%. However, the effects of low voltages on the lifetime of LiCs have not been evaluated.

Aging mechanisms in LiCs are still not well defined due to the absence of previous post-mortem studies. For this reason, the aim of this study is to apply different accelerated aging tests to LiCs, follow the evolution of the aging and then use post-mortem analyses to identify and compare aging mechanisms. The implemented tests were based on the floating aging that consists on maintaining the cells on a float charge at a certain voltage and at a constant temperature. Section 2 will describe the experimental conditions of the accelerated aging tests. Section 3 will present the physicochemical and electrochemical techniques used during the post-mortem studies. Section 4 will be then dedicated to the results of the post-mortem analyses. These results will be discussed in sections 5 and 6.

2. Experimental accelerated aging tests

Commercial LiCs made of an activated carbon positive electrode and a pre-lithiated graphite negative electrode were chosen to be tested in this study. This is the most common configuration of LiCs. These cells have an energy density of 13 Wh/kg and a power density of 10 kW/kg. At the positive electrode, the current collector is made of aluminum while at the negative electrode, a copper current collector is used. In the selected products, the pre-lithiation of the graphite electrode is done using the external short-circuit technique [23]. A sacrificial lithium metal electrode is inserted in the cell and connected through a copper current collector to the negative electrode. This external short-circuit between the negative electrode and the sacrificial electrode induces the migration of lithium ions in the electrolyte through the separator towards the negative electrode in which they intercalate. As a result, lithium metal completely disappears from the cell [24]. The pre-lithiation of the negative electrode aims to reduce the potential of the negative electrode in order to increase the total voltage of the cell [5], [25]. The conventional potential window of LiCs is between 2.2 V and 3.8 V. However, three characteristic values extracted from the operating principle of LiCs are

highlighted: 2.2 V, 3.0 V and 3.8 V [5], [25]. In fact, the open circuit voltage of the LiC is around 3 V [26]. When the cell is discharged from 3 to 2.2 V, lithium ions Li^+ are deintercalated from the pre-doped graphite negative electrode. They move towards the surface of the positive electrode where they accumulate [27]. On the other hand, when the cell is charged from 3 to 3.8 V, the anions of the electrolyte move towards the surface of the activated carbon and the cations intercalate into graphite layers of the negative electrode [28, 31]. Therefore, at 2.2, 3 and 3.8 V, the positive electrode of a LiC possesses different states.

In order to find the influence of the storage voltage on the lifetime of LiCs, accelerated aging tests based on the floating aging were realized. Detailed description of the tests that were done at 60°C and 70°C during 20 months can be found in [30]. In fact, eighteen samples were mounted in two different climatic chambers at 60°C and 70°C. The voltage constraint was ensured by power supplies connected to the cells during the whole aging process. Three voltage values were applied to different cells: 2.2, 3 and 3.8 V. Therefore, three samples per aging condition were assessed; one aging condition concerns one temperature and one voltage value. In order to follow the evolution of aging, periodic impedance spectroscopy measurement were done. Results showed that temperature increase accelerates aging of the cells since capacitance decrease and resistance increase were higher at 70°C than at 60°C. Concerning voltage effects, cells that aged at 2.2 V had the highest capacitance decrease (51 % at 60°C and 55 % at 70°C). At this storage voltage value, the double layer at the positive electrode is formed by lithium ions, the negative electronic charges and the anions PF_6^-. The negative electrode has the lowest state of charge at 2.2 V which is equivalent to the lowest amount of lithium ions intercalated in graphene layers [31]. On another hand, cells that aged at 3.0 V barely aged during the 20 months of floating aging. In fact, their capacitance decreased by around 2.5 % at 60°C and 7 % at 70°C. Their resistance increase was not significant as well, 4 % at 60°C and 6 % at 70°C [30]. At this voltage value, which is the open circuit voltage of the LiC right after its assembly, the positive electrode is at the neutral state while the state of charge of the negative electrode is higher than the one at 2.2 V. In addition, cells that aged at 3.8 V lost around 18 % of their capacitance at 60°C and 40 % at 70°C. However, their resistance increase was significant, reaching 95 % at 70°C and 60% at 60°C after 17 months of aging. As a result, swelling of these LiCs was noticed so their aging tests were interrupted after 17 months.

As can be seen from these results, storage voltage has a major influence on the aging of LiCs. Storing them at their lowest nominal voltage affects their capacitance while the highest voltage value affects their resistance. This indicates that aging mechanisms are different at each voltage value. In order to investigate the distinct degradations of the aged cells, post-mortem analyses were applied to three cells that aged at different voltage values. An additional brand new cell was disassembled as a reference cell for potential comparison.

3. Experimental post-mortem analyses

The four cells were disassembled in a glove box and free liquid electrolyte was collected from each one. The voltage of the aged cells was 2.2 V before disassembling while the one of the fresh cell was 3 V. No gassing was noticed for all cells, even the one that aged at 3.8 V and had significant swelling issues. The components of the cells were then retrieved to be analyzed and compared.

Physicochemical methods were selected according to the aging mechanisms involved. Figure 1 presents the sampling process and the post-mortem physicochemical techniques applied to each component of a LiC. An electrochemical analysis that aims to interpret the characteristics of each electrode separately was also employed. It is based on the assembly of symmetrical coin cells which contain two pellets of the same electrode, separated by appropriate electrolyte and separator. The evolution of electrode impedances with floating aging can then be depicted.

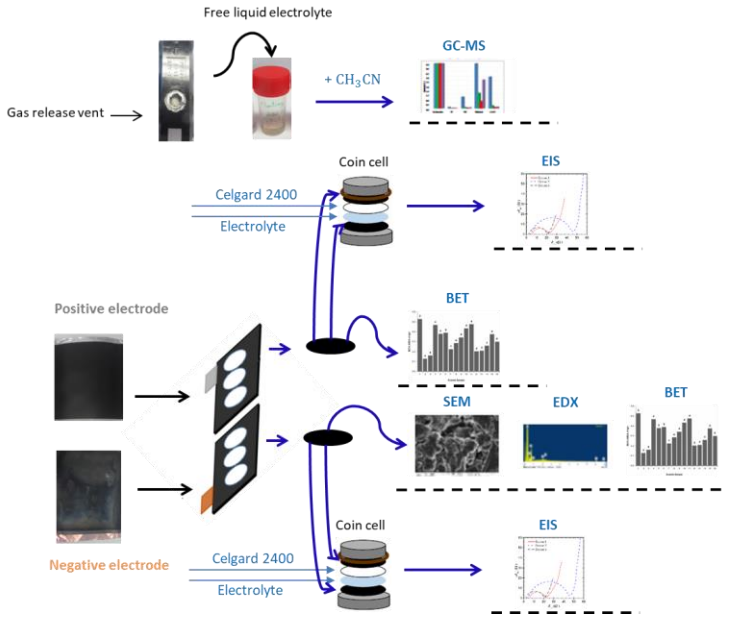

Figure 1. Overview of the components of LiCs, the extraction of samples and the applied post-mortem characterization techniques.

The electrolytes were analyzed using the GC-MS technique ('Gas Chromatography - Mass Spectrometry'). This method aims to separate volatile components of a sample in order to identify and then quantify them. The constituents of the electrolytes were identified by GC-MS technique. The GC-MS device having a 30 cm capillary column, an internal diameter of 0.25 mm and a 0.25 µm film was used. The temperature of the injector is 280°C. The injected sample was kept at an initial temperature of 40°C for 4 minutes and then the temperature increased at a rate of 10°C/min to 250°C where it was maintained for 2 minutes. Prior to the analysis, the samples were diluted five times in the same amount of acetonitrile (ACN), which is the most commonly employed carrier solvent of lithium-ion batteries electrolytes. Similar volumes of different samples were injected in the column.

The specific surfaces of the positive and negative electrodes were measured by the BET method (according to the model of Brunauer, Emmett and Teller). Scanning Electron Microscopy (SEM) combined with Energy-Dispersive X-ray microanalysis

(EDX) was applied to samples of the negative electrodes. The purpose of this technique is to reveal the structure of small objects with higher resolution than that of optical microscopes and to determine the chemical composition of the analyzed area [32].

Electrochemical analyses were also applied to the cells. The electrochemical measurements aim to isolate the two electrodes in order to determine their impedances separately. Electrodes are integrated in symmetrical coin cells that comprise a pellet of a given electrode in front of another pellet of the same electrode. Both pellets are separated by an electrolyte and two membranes of separators (Viledon in glass fibers and Celgard 2400 in polypropylene).

An interpretation of the results of the physicochemical and electrochemical analyses will be presented in the following section.

4. Results of post-mortem analyses

4.1 The electrolytes

The amount of free electrolyte retrieved from the four cells was approximately the same. However, the color significantly differed from one aging to another. The electrolyte of the fresh cell had a transparent color. On the other hand, the color became darker with the increase of the aging storage voltage.

The results of the GC-MS technique are presented in the chromatogram of figure 2.

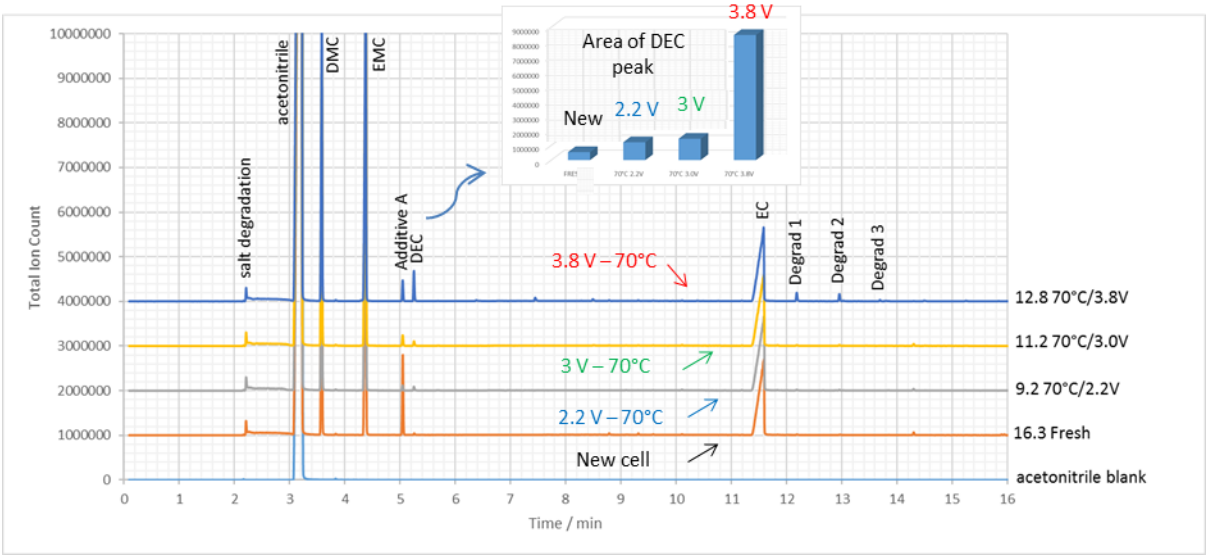

Figure 2. The evolution of ions total number with respect to the retention time of the four samples.

The components of the fresh electrolyte are identified as follows: EC/DMC/EMC (Ethylene Carbonate / Dimethyl carbonate / Ethyl methyl Carbonate) with a volume ratio of 25:27:48 (i.e. roughly %vol. EC/DMC/EMC v/v 1/1/2). Following the floating aging, the degradation of solvents and the appearance of numerous electrolyte degradation products are clearly observed, especially at 3.8 V. Moreover, an additional peak, corresponding to the DEC (Diethyl Carbonate) formation, appears. This is in agreement

with the literature, where DEC and DMC have already been observed by transesterification of EMC [33]–[35]. Three small peaks related to carbonate degradation products are also detected between 12 and 14 minutes, especially at 3.8 V. Several solvent decomposition reactions can cause the generation of these products. For example, a reduction reaction of DEC and EMC can lead to the formation of an alkoxide, which can contribute to the formation of a dialkyl carbonate [35].

The amount of additive A that appears at 5.05 minutes varies with aging conditions. This component could also be an impurity. In fact, it is consumed during the floating aging tests, especially at 2.2 V. However, it has not been identified. By enlarging the spectrum of figure 2, additional degradation products are observed such as the diethyl fluorophosphate, which could be a degradation product of $LiPF_6$ salt.

The ionic conductivity was determined by sandwiching SS/electrolyte/SS (Stainless Steel (SS) blocking electrodes) cells at room temperature. Results of the measurements are shown in Table 1. The conductivity did not significantly change after aging for the cell that aged at 3.0 V. As a result, one can deduce that the amount of salt present in the electrolyte was not consumed. On the other hand, the ionic conductivity of the electrolyte depends on the lithium salt concentration and on the mixture of solvents [36], [37]. The composition of the electrolyte did not significantly change with aging. The electrolyte is mainly composed of EC/DMC/EMC 1:1:2. However, even a small change in this ratio can affect the value of the ionic conductivity. Therefore, one can relate the increase of the ionic conductivity of cells that aged at 2.2 and 3.8 V to a small change of the ratio between solvents. Moreover, the presence of DEC in the electrolyte of the cell that aged at 3.8 V can contribute to this enhancement of ionic conductivity [36].

Table 1. Comparison of the conductivities of the electrolytes extracted from the new cell and from the aged ones.

		Aged cells at 70°C		
	Brand new cell	2.2 V	3.0 V	3.8 V
Conductivity ($mS.cm^{1}$)	9.5	11.0	9.6	11.0

4.2 The negative electrodes

The most common aging mechanism of a graphite negative electrode is the growth of the SEI layer on its surface. Visual inspections of the negative electrodes derived from the fresh cell and the aged ones are given in Table 2.

Table 2. Visual inspections of the negative electrodes of LiCs after calendar aging tests at 70°C during 20 months for cells that aged at 2.2 V and 3.0 V, and during 17 months for cells that aged at 3.8 V. Voltage values before dissembling are the following: 3 V for the brand new cell and 2.2 V for the aged ones.

		Observations on the graphite based anode
	Brand new cell	• Lithiated electrode whose surface shows different colored areas varying from brown to grey.
Aged cells at 70°C	2.2 V	• Lithiated electrode whose surface shows different inhomogeneous colored areas varying between blue and red, which indicates that the degrees of lithiation of surface particles are different. • Delamination of the electrode material from the current collector especially at the folded areas.
	3 V	• Lithiated electrode whose surface shows different inhomogeneous colored areas varying between dark blue and brown, which indicates that the degrees of lithiation of surface particles are different. • Delamination of the electrode material from the current collector especially at the folded areas. • Presence of few areas with visible white deposits.
	3.8 V	• Lithiated electrode whose surface shows more homogenous colored areas varying between blue and brown. • More frequent delamination of the electrode material from the current collector especially at the folded areas. • Presence of several extended areas with visible white deposits.

The coloration of the negative electrode depends on its degree of lithiation (blue for LiC_{18}, red for LiC_{12} and gold for LiC_6 [38]). According to the results presented in table 2, the aging storage voltage has a very important impact on the degradation of the negative electrode. In fact, during disassembling, the higher the storage voltage is, the higher the delamination of active material from the current collector (that consists of a copper mesh) becomes. This reflects a loss in the adhesion between the collector and

the active material. At a certain stage, the copper becomes visible in some areas. In fact, when the SEI layer grows at the surface of the negative electrode, chemical reactions can be induced between the separator and the electrode, causing the detachment of the current collector during the opening of the cell and the separation of the separator from the electrode. Moreover, the color of the electrode surfaces changes. Despite the fact that chemical changes in the SEI layer are not assessed at this stage, color changes may indicate changes in the thickness or the chemistry of the material [39].

Lithium deposition, which appears slightly for cells aging at 3.0 V and more frequently for cells aging at 3.8 V, was not expected. In fact, for negative electrodes of lithium-ion batteries, this aging mechanism is mainly encountered during their cycling or during their operation at a specific current at low temperatures [13]. In [32], commercial NMC (Nickel Manganese Cobalt) lithium-ion cells, 16 Ah, that underwent calendar aging tests at 45°C and 60°C, exhibited a white deposit at the negative electrode. This was revealed during their post-mortem studies. The corresponding tests included periodic galvanostatic characterizations. Other tests were then conducted without the periodic characterizations. As a result, no lithium deposits were noticed on the negative electrodes of these cells. Therefore, the results showed that the lithium deposit was due to the periodic galvanostatic characterizations since the same phenomenon was not found during the tests without periodic interruptions. During the accelerated aging tests of this study, there was no galvanostatic charging and discharging of the cells. Only periodic impedance spectroscopy measurements were applied to LiCs. Therefore, the initial and final characterizations could be the reason behind the formation of the visible lithium metal on the surface of their negative electrodes. These characterizations are based on the standard protocol of charging a LiC by a constant current, maintaining its voltage constant by a float charge at 3.8 V for 30 minutes, then discharging it to 2.2 V by a constant current [25].

In order to analyze the growth of the SEI layer on the surface of the aged negative electrodes, their mass was measured and compared to that of the fresh negative electrode. Thus, six pellets per electrode were washed with DMC and then dried. Their mass was measured with a balance having an accuracy of +/- 0.1 mg. The mass measurements were carried out in the glove box to prevent the electrodes from gaining weight with humidity and the surface from reacting with the air. The percentages of mass increase (m (%)) measured at the interface (at the beginning of the unwinding of the negative electrode), in the middle and at the center (at the end of the complete unwinding of the assembly) of the winding are present in table 3. The mass of the negative electrode increases with the increase of the aging voltage. This is an indicator of the growth of the SEI layer with voltage increase, in accordance with visual inspections.

Table 3. The increase of electrodes mass measured at three different locations.

	m (%)		
Calendar aging condition at 70°C	Interface	Middle	Center

2.2 V	0	0.2	0.3
3 V	0.9	1.5	0.7
3.8 V	1.2	3.1	1.4

Surfaces of electrodes were observed using SEM in order to visualize the morphology of surface materials. SEM is often combined with EDX analysis for determining the chemical composition of the studied area [40]. The samples were transferred to the SEM measurement tool through an adequate chamber in order to avoid their exposure to the air. Figure 3 shows images taken by the SEM of the negative electrodes of graphite extracted from the brand new cell and the aged ones under different conditions.

The graphite based electrode extracted from the cell that aged at 2.2 V has a surface quite similar to the fresh electrode. Nevertheless, few scattered filaments can be seen on the surface. In the image corresponding to the cell that aged at 3.0 V, the particles appear to be covered by a surface layer. There are areas containing a filament-shaped white deposit. As for the cell that aged at 3.8 V, the surface of its negative electrode has filament deposits as well. However, they do not cover the surface and are not visible on a macroscopic scale. Zones with particles having an iridescent effect are also observed.

Table 4 presents the percentage of each element detected by the EDX for all samples. At 3.0 and 3.8 V, the fluorine level increases showing a possible formation of LiF. Areas with a white deposit have a significant percentage of fluorine. The aluminum appears in the iridescent areas that can be observed on the surface of the negative electrode from the cell that aged at 3.8 V. This indicates the degradation of the positive current collector of the LiC and the migration of particles to the negative electrode where they are reduced. Another source of aluminum can be the separator that is covered with a layer of alumina. Some particles of alumina could be detached from the separator and adhered on the negative electrode of the cell that aged at 3.8 V. In order to investigate the origin of the aluminum, the SEM-EDX data of the electrode were observed. The aluminum was detected in all EDX analyzes that were performed on four different zones of the electrode. On the other hand, the quantity of aluminum was more important on a distinct particle. This particle could actually be a particle of alumina. However, since aluminum is also detected on the other zones of the electrode, without the presence of this type of particles, one can conclude that aluminum generated from the corrosion of the current collector is detected. In addition, during the disassembly of the cell, the positive electrode was more fragile than the other electrode. This may be caused by the oxidation of the aluminum current collector and its deposition on the negative electrode.

BET surface measurements were also applied to the negative electrodes. The results are present in table 5.

Fresh electrode of lithiated graphite

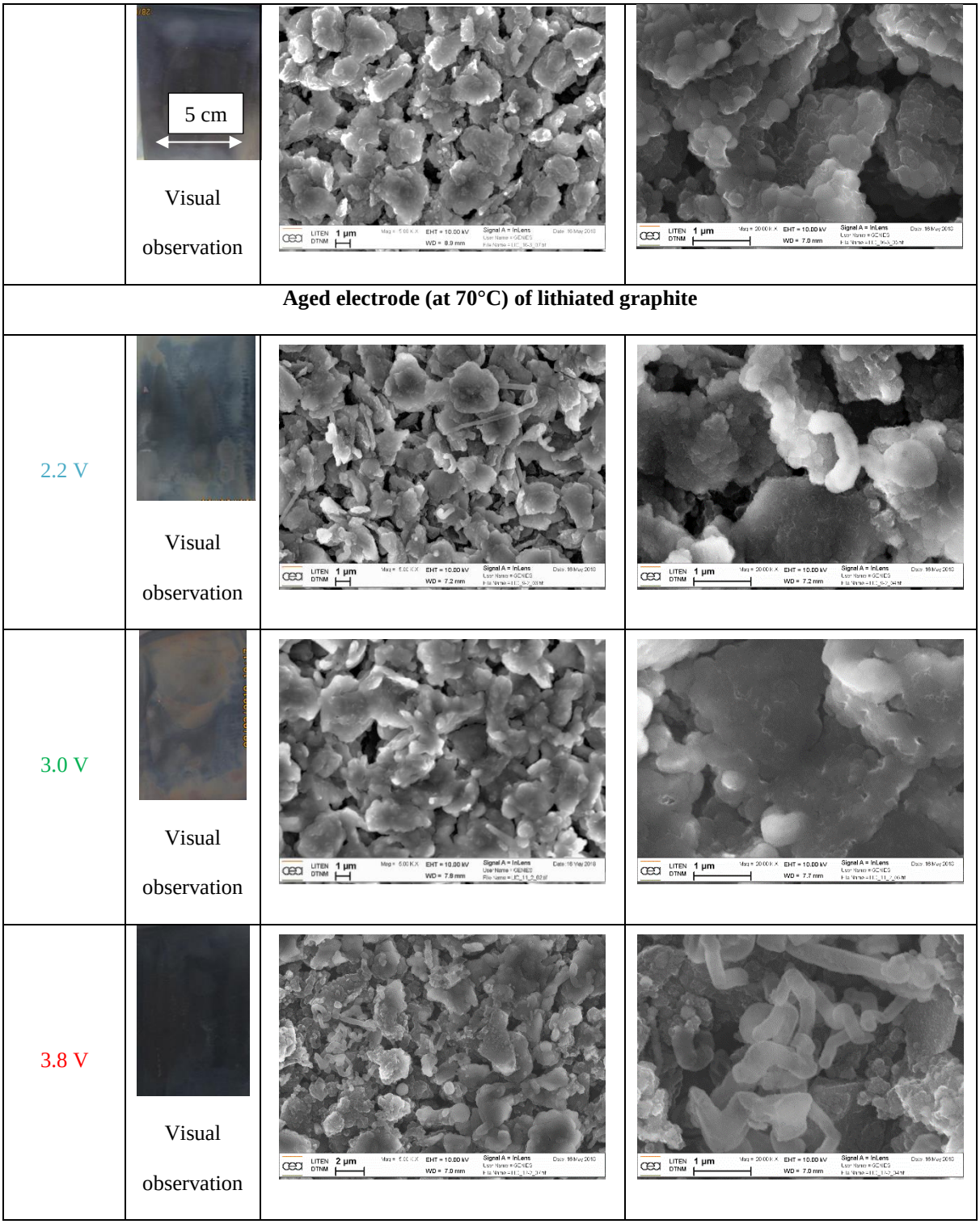

Figure 3. Comparison of SEM images of the negative electrodes extracted from the brand new cell and the cells aged at 70°C.

Table 4. Percentage of each element detected by SEM/EDX applied on samples of graphite electrodes extracted from the fresh cell and the aged ones.

Element			C	F	O	P	S	Al
% at.	Brand new cell		84.2	10.28	4.9	0.48	0.15	X
		2.2 V	91.45	3.44	4.36	0.53	0.22	X

	Aged cells at 70°C	3 V	75.38	15.67	8.06	0.69	0.2	X
		3.8 V	71.22	17.22	10.09	0.85	0.26	0.37

Table 5. Comparison of specific surfaces of the negative electrodes.

		Aged cells at 70°C		
	Brand new cell	2.2 V	3 V	3.8 V
BET surface (m^2/g)	4.55	6.06	3.94	7.84

The surfaces of the electrodes that aged at 2.2 and 3.8 V increase during aging while the one of the electrode that aged at 3 V decreases. According to figure 3, many deposits in the form of filaments or zones with different visual aspects are found on the negative electrode extracted from the cell that aged at 3.8 V. Same applies for the negative electrode originating from the cell that aged at 2.2 V, but with a less rate. This may explain the increase of the surface. In this case, new surfaces are created. On the other hand, for the electrode extracted from the cell that aged at 3 V, it can be observed that in certain areas of the electrode, the particles are covered by a layer, which explains the decrease of the BET surface. As a result, the irreversible loss of lithium ions from the negative electrode induces the decrease of the capacity of LiCs, which is noticed for cells aging at 2.2 and 3.8 V.

4.3 The positive electrodes

According to the literature, the main aging mechanism of the positive electrode is the pore blocking of the activated carbon due to parasitic reactions between the functional groups present on its surface and the components of the electrolyte [2], [15]. This phenomenon is not visible on a macroscopic scale because of nanoscale porosity. In fact, the visual inspections do not reveal differences between the surfaces of the fresh electrode and the aged ones. Nevertheless, during the dismounting of the cell that aged at 3.8 V, it was found that the positive electrode was very fragile. A significant delamination of the active material from the current collector was noticed. In addition, the separator facing this electrode had a brownish color and its membrane was significantly adherent. This could be due to the thermal and electrochemical degradation of $LiPF_6$. In fact, in [42], the thermal stabilities of two electrolytes containing the same solvent but different salts, $LiPF_6$ and $LiN(SO_2C_2F_5)_2$, were compared. Visual inspections showed that only the color of the electrolyte containing $LiPF_6$ changed at high temperatures. It became gradually darker at increasing temperatures such as 60°C. These interpretations can be the reason behind the strong increase of the series resistance of cells aged at 3.8 V.

BET surface measurements (Nitrogen at 77K) were applied to the positive electrodes after washing them in a Soxhlet extractor

for 48 hours with ACN and then scraping them. The results are present in table 6.

Table 6. Comparison of the specific surface areas of the positive electrodes.

		Aged cells at 70°C		
	Brand new cell	2.2 V	3.0 V	3.8 V
BET surface (m^2/g)	1341	1199	1375	1156

The active surfaces of the positive electrodes of the cells aged at 2.2 and 3.8 V decrease after aging, showing a potential pore blocking. As a result, their respective capacities also decrease. As previously seen, capacities of the negative electrodes also decrease because of the loss of cyclable lithium ions. These post-mortem analyses are therefore consistent with the observed loss of capacitance of cells that aged at 2.2 and 3.8 V.

In order to analyze the electrochemical characteristics of the electrodes, symmetrical coin cells were manufactured according to the protocol explained in the following paragraph.

4.4 Electrochemical analyses

The impedances of the manufactured coin cells were measured using Electrochemical Impedance Spectroscopy (EIS) over a frequency range from 100 mHz to 100 kHz with an excitation amplitude of 5mV. The cells were completely discharged to 0 V before the measurement. Nyquist diagrams of four coin cells formed by positive electrodes from the four disassembled LiCs are shown in figure 4.

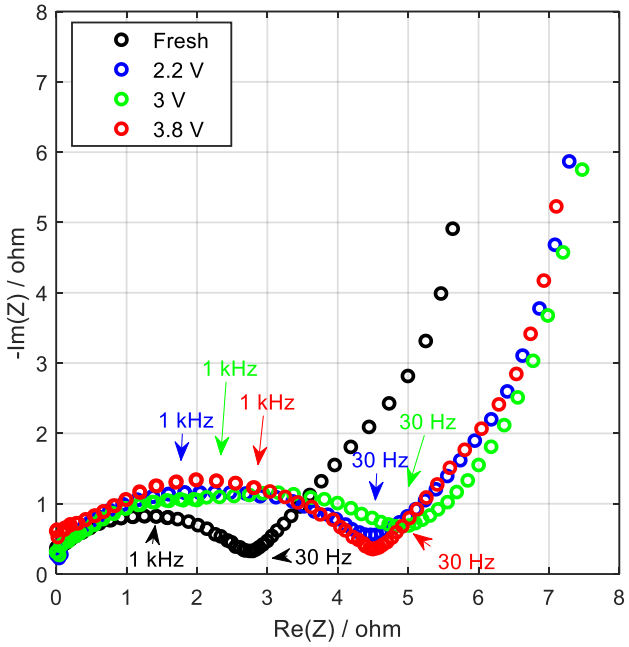

Figure 4. Comparison of Nyquist diagrams of symmetric coin cells at 0 V, each one formed by pellets from a positive electrode of a disassembled LiC.

The Nyquist diagrams of the aged electrodes do not show any major difference between them. However, comparing them to the Nyquist diagram of the fresh positive electrode, it can be concluded that the resistance of the electrodes has increased as the values of the real parts of the impedance are higher after aging.

Figure 5 shows the Nyquist diagrams of four coin cells formed by the negative electrodes extracted from the four disassembled LiCs.

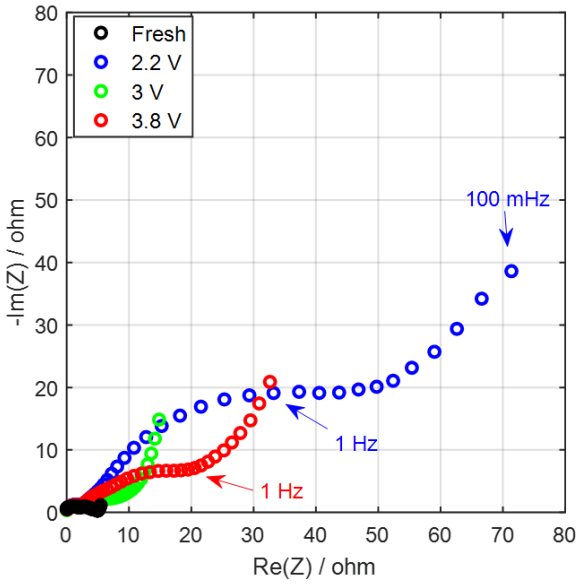

Figure 5. Comparison of Nyquist diagrams of symmetric coin cells at 0 V, formed by pellets from a negative electrode of a disassembled LiC.

The Nyquist diagrams of the three aged cells clearly differ from the Nyquist diagram of the fresh cell. The greatest difference is observed for the electrode of the cell that aged at 2.2 V. On the other hand, the previous post-mortem analyzes did not show any major damage to the surface of this electrode. In order to better understand the changes that affect the negative electrode at different voltages, figure 6 shows two enlargements of the Nyquist diagrams at medium and high frequencies.

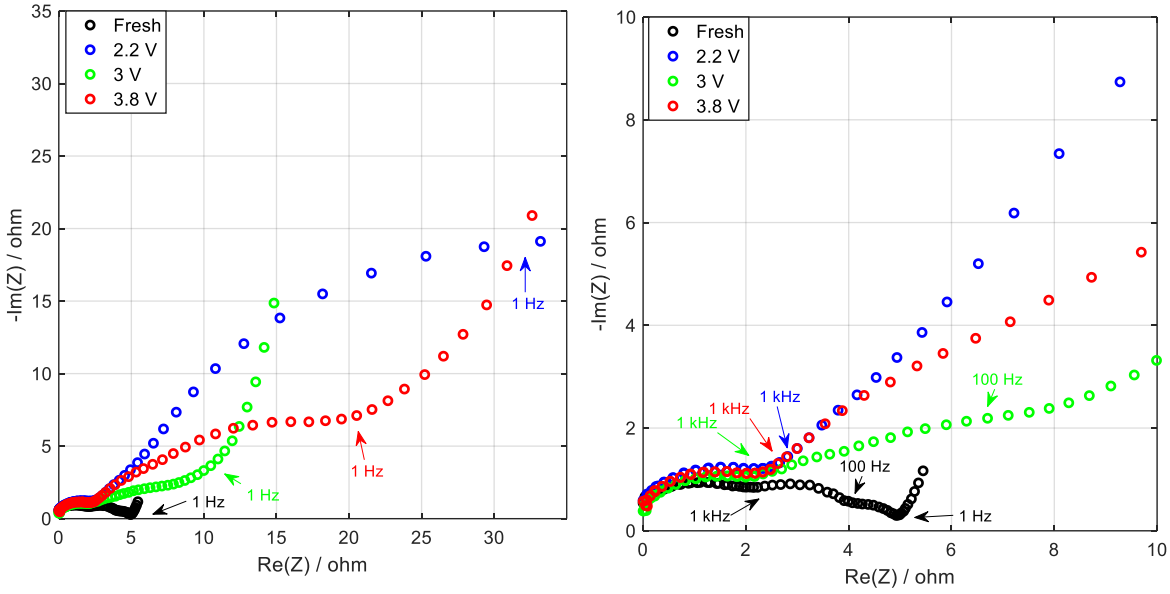

Figure 6. Enlargement scale of Nyquist diagrams of symmetrical button cells, formed by pellets from a negative electrode of a disassembled LiC.

The Nyquist diagram of the fresh electrode corresponds to the diagram of a completely lithiated graphite electrode [43]. Three semi-circles appear in this diagram: the first one at high frequencies (above 1 kHz) corresponds to interactions between the current collector and the particles, the second one at medium frequencies is related to the SEI (between 1 kHz and 100 Hz) and the third one at low frequencies (between 100 Hz and 1 Hz) is related to charge transfer. The size of second and third semicircles is reduced at the end of the lithiation, which reflects the behavior of the graphite electrode extracted from a fresh LiC. The Nyquist diagrams of the aged electrodes present only two semicircles. The first semicircle is not affected by aging while the second one becomes larger showing an increase of the resistance due to the SEI. The third semicircle disappears indicating a potential drift of the negative electrode due the rise of the charge transfer resistance [43]. The potential drift is mainly attributed to an irreversible loss of lithium ions. Therefore, the negative electrode of the LiC aged at 2.2 V has lost more cyclable lithium ions than the one of the LiC aged at 3.8 V. However, according to the previous post-mortem analysis on the negative electrode of LiC aged at 2.2 V, no important modification of the SEI layer was reported. The morphology of its surface and its chemical composition were not affected by aging. Therefore, this potential drift of the negative electrode can be related to an irreversible adsorption of lithium ions by the functional groups present on the surface of the positive electrode. In fact, according to the operating principle of a LiC, at 2.2 V, lithium ions accumulate at the surface of the positive electrode. The parasitic groups present at the surface of the positive activated carbon electrode could irreversibly adsorb these cations Li^+ inducing the decrease of its performance [30], [44], [45]. A clear explanation of this phenomenon is still missing in the literature [44], [45]. SEI layer growth was mainly observed on the negative electrodes of cells aged at 3.0 and 3.8 V. This phenomenon can be the main cause of the increase of the potential of their electrodes generating such evolutions of their Nyquist diagram.

5. Discussion

Due to the hybrid composition of LiCs, aging mechanisms strongly depend on their state of charge (reflected by their terminal voltage). According to accelerated aging tests applied to these new devices, two main mechanisms whose origins differ from one voltage to another can be highlighted:

- the loss of lithium ions pre-intercalated in the negative electrode,
- the pore blocking at the positive electrode.

The pore blocking of the of the positive electrode results in a decrease in the value of the capacitance. At 2.2 V, the products of the reactions between the lithium ions and the functional groups present on the surface of the positive electrode block its pores. At 3.8 V, the reaction products between electrolyte components that decompose at high temperatures and the functional groups also cause pore blocking. Since at 3.0 V the positive electrode of a LiC is at the approximate neutral state [30], the pore blocking is less pronounced at this voltage value.

The loss of the cyclable lithium ions of the negative electrode causes the drift of its potential. As a result, the total capacity of the LiC decreases because of capacity decrease of the negative electrode, causing a limitation of the use of the total capacity of the positive electrode. If the LiCs are stored at 2.2 V, this loss of capacity is caused by the potential drift of the positive electrode, which irreversibly adsorbs the lithium ions. This requires additional deintercalation of lithium ions from the negative electrode. On the other hand, if the LiCs are stored at 3.8 V, the growth of the SEI layer on the surface of the negative electrode is the reason behind the loss of capacity. This aging mechanism is also found for the cell that aged at 3.0 V but with less damage to its performance.

In a LiC, these two mechanisms are complementary. Consequently, their respective effects accelerate the degradation of the two electrodes. According to the post-mortem analyses, other degradations have been noticed such as the decomposition of the electrolyte and the degradation of the positive current collector. Figure 7 summarizes the aging mechanisms as a function of the voltage of the LiC.

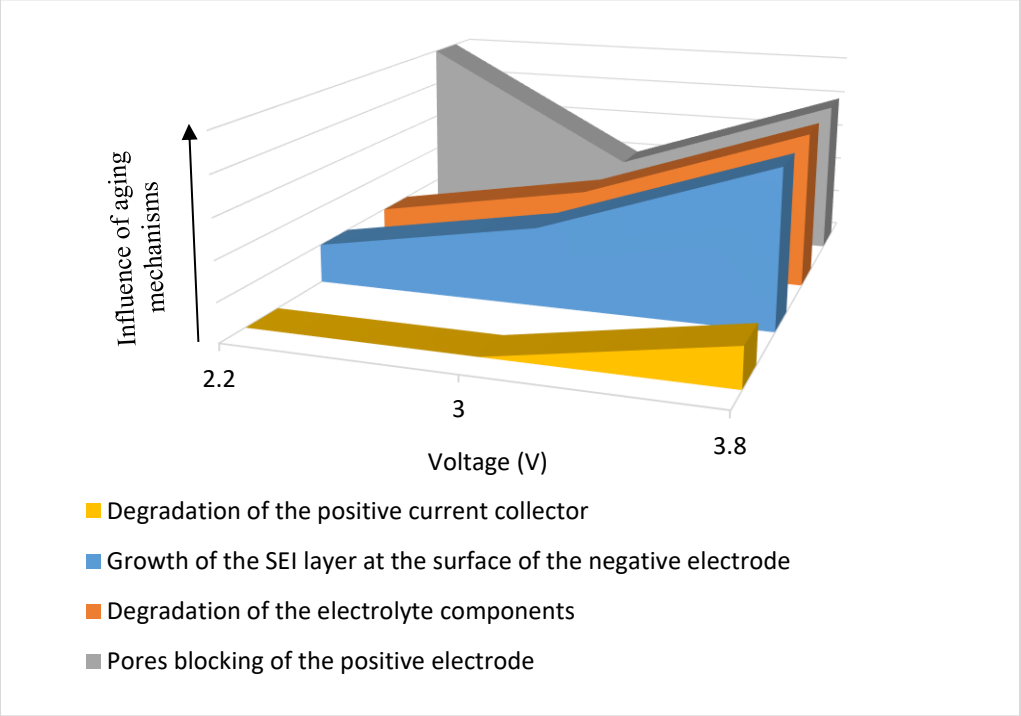

Figure 7. Summary of aging mechanisms with respect to the storage voltage of the LiC.

6. Conclusion

Even though the anode of the LiCs is similar to the anode of lithium-ion batteries, the structure and the aging of LiCs are not similar to the ones of lithium-ion batteries. For the majority of LiBs, the highest the calendar voltage is, the stronger the aging becomes. This was not found in LiCs whose capacitance decreases at 2.2 V at a higher rate than at 3.8 V. This difference is mainly related to their positive electrode made of activated carbon. Therefore, a unique post-mortem study was done on LiCs that aged at three different voltage values and 70°C during 20 months. Conventional characterization techniques were applied to the aged cells.

Aging mechanisms that depend on the state of charge of a LiC were revealed for the first time in the literature. The decrease of the capacitance values were related to the pore blocking at the positive electrode and / or the potential drift of the negative electrode. This latter mechanism is caused by the loss of pre-intercalated lithium ions in the negative electrode. At 2.2 V, the loss was due to an irreversible adsorption of lithium ions by the functional groups present at the surface of the positive electrode. However, at 3.8 V, the loss was related to the growth of the SEI layer at the surface of the negative electrode. In addition, the degradation of the electrolyte accelerated with the increase of the voltage. A decomposition of the positive current collector was observed only at 3.8 V.

At 3.0 V, the main aging mechanisms were the growth of the SEI layer at the graphite electrode and the degradation of electrolytes components. However, their effects did not cause to the complete deterioration of the cell. Even after 20 months of aging, the performance of the cell was still acceptable.

In order to improve the lifetime of LiCs, an electrochemical analysis concerning the irreversible adsorption of lithium ions by the functional groups that reside on the surface of the activated carbon should be performed. This phenomenon, which is not studied in details in the literature, is responsible for a major degradation of LiCs. A potential solution to avoid this aging mechanism would improve the operation of this new technology.

References

[1] E. Redondo-Iglesias, P. Venet, et S. Pelissier, « Calendar and cycling ageing combination of batteries in electric vehicles », *Microelectronics Reliability*, vol. 88-90, p. 1212-1215, sept. 2018, doi: 10.1016/j.microrel.2018.06.113.

[2] R. German, P. Venet, A. Sari, O. Briat, et J. M. Vinassa, « Improved Supercapacitor Floating Ageing Interpretation Through Multipore Impedance Model Parameters Evolution », *IEEE Transactions on Power Electronics*, vol. 29, nº 7, p. 3669-3678, juill. 2014, doi: 10.1109/TPEL.2013.2279428.

[3] B. Stiaszny, J. C. Ziegler, E. E. Krauß, J. P. Schmidt, et E. Ivers-Tiffée, « Electrochemical characterization and post-mortem analysis of aged LiMn2O4–Li(Ni0.5Mn0.3Co0.2)O2/graphite lithium ion batteries. Part I: Cycle aging », *Journal of Power Sources*, vol. 251, p. 439-450, avr. 2014, doi: 10.1016/j.jpowsour.2013.11.080.

[4] Y. Gao, J. Jiang, C. Zhang, W. Zhang, Z. Ma, et Y. Jiang, « Lithium-ion battery aging mechanisms and life model under different charging stresses », *Journal of Power Sources*, vol. 356, p. 103-114, juill. 2017, doi: 10.1016/j.jpowsour.2017.04.084.

[5] N. E. Ghossein, A. Sari, et P. Venet, « Interpretation of the Particularities of Lithium-Ion Capacitors and Development of a Simple Circuit Model », in *2016 IEEE Vehicle Power and Propulsion Conference (VPPC)*, oct. 2016, p. 1-5, doi: 10.1109/VPPC.2016.7791712.

[6] J. Ronsmans et B. Lalande, « Combining energy with power: Lithium-ion capacitors », in *2015 International Conference on Electrical Systems for Aircraft, Railway, Ship Propulsion and Road Vehicles (ESARS)*, mars 2015, p. 1-4, doi: 10.1109/ESARS.2015.7101494.

[7] J. Vetter *et al.*, « Ageing mechanisms in lithium-ion batteries », *Journal of Power Sources*, vol. 147, nº 1, p. 269-281, sept. 2005, doi: 10.1016/j.jpowsour.2005.01.006.

[8] A. Barré, B. Deguilhem, S. Grolleau, M. Gérard, F. Suard, et D. Riu, « A review on lithium-ion battery ageing mechanisms and estimations for automotive applications », *Journal of Power Sources*, vol. 241, p. 680-689, nov. 2013, doi: 10.1016/j.jpowsour.2013.05.040.

[9] P. Verma, P. Maire, et P. Novák, « A review of the features and analyses of the solid electrolyte interphase in Li-ion batteries », *Electrochimica Acta*, vol. 55, nº 22, p. 6332-6341, sept. 2010, doi: 10.1016/j.electacta.2010.05.072.

[10] E. Peled, D. Golodnitsky, et G. Ardel, « Advanced Model for Solid Electrolyte Interphase Electrodes in Liquid and Polymer Electrolytes », *J. Electrochem. Soc.*, vol. 144, nº 8, p. L208-L210, août 1997, doi: 10.1149/1.1837858.

[11] M. N. Richard et J. R. Dahn, « Accelerating Rate Calorimetry Study on the Thermal Stability of Lithium Intercalated Graphite in Electrolyte. I. Experimental », *J. Electrochem. Soc.*, vol. 146, nº 6, p. 2068-2077, juin 1999, doi: 10.1149/1.1391893.

[12] « Mechanism of self-discharge in graphite–lithium anode - ScienceDirect ». https://www-sciencedirect-com.docelec.univ-lyon1.fr/science/article/pii/S0013468601008271 (consulté le mars 15, 2018).

[13] C. Lin, A. Tang, H. Mu, W. Wang, et C. Wang, « Aging Mechanisms of Electrode Materials in Lithium-Ion Batteries for Electric Vehicles », *Journal of Chemistry*, 2015. https://www.hindawi.com/journals/jchem/2015/104673/ (consulté le févr. 28, 2018).

[14] R. Richner, S. Müller, et A. Wokaun, « Grafted and crosslinked carbon black as an electrode material for double layer capacitors », *Carbon*, vol. 40, nº 3, p. 307-314, mars 2002, doi: 10.1016/S0008-6223(01)00100-2.

[15] P. Azaïs *et al.*, « Causes of supercapacitors ageing in organic electrolyte », *Journal of Power Sources*, vol. 171, nº 2, p. 1046-1053, sept. 2007, doi: 10.1016/j.jpowsour.2007.07.001.

[16] N. N. Mohammad Naim, « Modelling the ageing behaviour of supercapacitors using electrochemical impedance spectroscopy for dynamic applications », juill. 25, 2015. http://eprints.nottingham.ac.uk/29169/ (consulté le mars 17, 2018).

[17] S. Dsoke, B. Fuchs, E. Gucciardi, et M. Wohlfahrt-Mehrens, « The importance of the electrode mass ratio in a Li-ion capacitor based on activated carbon and Li4Ti5O12 », *Journal of Power Sources*, vol. 282, p. 385-393, mai 2015, doi: 10.1016/j.jpowsour.2015.02.079.

[18] P. Keil *et al.*, « Calendar Aging of Lithium-Ion Batteries I. Impact of the Graphite Anode on Capacity Fade », *J. Electrochem. Soc.*, vol. 163, nº 9, p. A1872-A1880, janv. 2016, doi: 10.1149/2.0411609jes.

[19] X. Sun *et al.*, « Electrochemical performances and capacity fading behaviors of activated carbon/hard carbon lithium ion capacitor », *Electrochimica Acta*, vol. 235, p. 158-166, mai 2017, doi: 10.1016/j.electacta.2017.03.110.

[20] M. Schroeder, M. Winter, S. Passerini, et A. Balducci, « On the cycling stability of lithium-ion capacitors containing soft carbon as anodic material », *Journal of Power Sources*, vol. 238, p. 388-394, sept. 2013, doi: 10.1016/j.jpowsour.2013.04.045.

[21] T. Aida, I. Murayama, K. Yamada, et M. Morita, « Analyses of Capacity Loss and Improvement of Cycle Performance for a High-Voltage Hybrid Electrochemical Capacitor », *J. Electrochem. Soc.*, vol. 154, nº 8, p. A798-A804, août 2007, doi: 10.1149/1.2746562.

[22] M. Uno et A. Kukita, « Cycle Life Evaluation Based on Accelerated Aging Testing for Lithium-Ion Capacitors as Alternative to Rechargeable Batteries », *IEEE Transactions on Industrial Electronics*, vol. 63, nº 3, p. 1607-1617, mars 2016, doi: 10.1109/TIE.2015.2504578.

[23] M. Kim *et al.*, « A fast and efficient pre-doping approach to high energy density lithium-ion hybrid capacitors », *J. Mater. Chem. A*, vol. 2, nº 26, p. 10029-10033, juin 2014, doi: 10.1039/C4TA00678J.

[24] G. G. Amatucci, U.S. Patent No. 6,252,762, Washington, DC: U.S. Patent and Trademark Office, 2001.

[25] N. E. Ghossein, A. Sari, et P. Venet, « Nonlinear Capacitance Evolution of Lithium-Ion Capacitors Based on Frequency- and Time-Domain Measurements », *IEEE Transactions on Power Electronics*, vol. 33, nº 7, p. 5909-5916, juill. 2018, doi: 10.1109/TPEL.2017.2745716.

[26] S. R. Sivakkumar et A. G. Pandolfo, « Evaluation of lithium-ion capacitors assembled with pre-lithiated graphite anode and activated carbon cathode », *Electrochimica Acta*, vol. 65, p. 280-287, mars 2012, doi: 10.1016/j.electacta.2012.01.076.
[27] W. Cao, "Novel High Energy Density Li-Ion Capacitors," Phd thesis, Florida State University, 2013.
[28] S. R. Sivakkumar, V. Ruiz, and A. G. Pandolfo, "Assembly and testing of lithium-ion capacitors," 2010.
[29] A. Shellikeri, I. Hung, Z. Gan, et J. Zheng, « In Situ NMR Tracks Real-Time Li Ion Movement in Hybrid Supercapacitor–Battery Device », *J. Phys. Chem. C*, vol. 120, nº 12, p. 6314-6323, mars 2016, doi: 10.1021/acs.jpcc.5b11912.
[30] N. E. Ghossein, A. Sari, et P. Venet, « Effects of the Hybrid Composition of Commercial Lithium-Ion Capacitors on Their Floating Aging », *IEEE Transactions on Power Electronics*, vol. 34, nº 3, p. 2292-2299, mars 2019, doi: 10.1109/TPEL.2018.2838678.
[31] A. Shellikeri, I. Hung, Z. Gan, et J. Zheng, « In Situ NMR Tracks Real-Time Li Ion Movement in Hybrid Supercapacitor–Battery Device », *J. Phys. Chem. C*, vol. 120, nº 12, p. 6314-6323, mars 2016, doi: 10.1021/acs.jpcc.5b11912.
[32] B. Pilipili Matadi, *Etude des mécanismes de vieillissement des batteries Li-ion en cyclage à basse température et en stockage à haute température : compréhension des origines et modélisation du vieillissement*. Grenoble Alpes, 2017.
[33] H. Yoshida, T. Fukunaga, T. Hazama, M. Terasaki, M. Mizutani, et M. Yamachi, « Degradation mechanism of alkyl carbonate solvents used in lithium-ion cells during initial charging », *Journal of Power Sources*, vol. 68, nº 2, p. 311-315, oct. 1997, doi: 10.1016/S0378-7753(97)02635-9.
[34] G. Gachot *et al.*, « Deciphering the multi-step degradation mechanisms of carbonate-based electrolyte in Li batteries », *Journal of Power Sources*, vol. 178, nº 1, p. 409-421, mars 2008, doi: 10.1016/j.jpowsour.2007.11.110.
[35] H. Kim, S. Grugeon, G. Gachot, M. Armand, L. Sannier, et S. Laruelle, « Ethylene bis-carbonates as telltales of SEI and electrolyte health, role of carbonate type and new additives », *Electrochimica Acta*, vol. 136, p. 157-165, août 2014, doi: 10.1016/j.electacta.2014.05.072.
[36] D. Yaakov, Y. Gofer, D. Aurbach, et I. C. Halalay, « On the Study of Electrolyte Solutions for Li-Ion Batteries That Can Work Over a Wide Temperature Range », *J. Electrochem. Soc.*, vol. 157, nº 12, p. A1383, nov. 2010, doi: 10.1149/1.3507259.
[37] J. Yamaki, « SECONDARY BATTERIES – LITHIUM RECHARGEABLE SYSTEMS – LITHIUM-ION | Overview », in *Encyclopedia of Electrochemical Power Sources*, J. Garche, Éd. Amsterdam: Elsevier, 2009, p. 183-191.
[38] Y. Qi et S. J. Harris, « In Situ Observation of Strains during Lithiation of a Graphite Electrode », *J. Electrochem. Soc.*, vol. 157, nº 6, p. A741-A747, juin 2010, doi: 10.1149/1.3377130.
[39] L. Somerville, « Post-mortem analysis of lithium-ion cells after accelerated lifetime testing. », PhD thesis, University of Warwick, 2017.
[40] T. Waldmann *et al.*, « Review—Post-Mortem Analysis of Aged Lithium-Ion Batteries: Disassembly Methodology and Physico-Chemical Analysis Techniques », *J. Electrochem. Soc.*, vol. 163, nº 10, p. A2149-A2164, janv. 2016, doi: 10.1149/2.1211609jes.
[41] M. Winter, P. Novák, et A. Monnier, « Graphites for Lithium-Ion Cells: The Correlation of the First-Cycle Charge Loss with the Brunauer-Emmett-Teller Surface Area », *J. Electrochem. Soc.*, vol. 145, nº 2, p. 428-436, févr. 1998, doi: 10.1149/1.1838281.
[42] G. Nagasubramanian, « Comparison of the thermal and electrochemical properties of LiPF6 and LiN(SO2C2F5)2 salts in organic electrolytes », *Journal of Power Sources*, vol. 119-121, p. 811-814, juin 2003, doi: 10.1016/S0378-7753(03)00246-5.
[43] S. Chhor, « Etude et modélisation de l'interface graphite/électrolyte dans les batteries lithium-ion », PhD thesis, University of Grenoble, 2014.
[44] P. W. Ruch, D. Cericola, M. Hahn, R. Kötz, et A. Wokaun, « On the use of activated carbon as a quasi-reference electrode in non-aqueous electrolyte solutions », *Journal of Electroanalytical Chemistry*, vol. 636, nº 1, p. 128-131, nov. 2009, doi: 10.1016/j.jelechem.2009.09.007.
[45] M. Widmaier *et al.*, « Carbon as Quasi-Reference Electrode in Unconventional Lithium-Salt Containing Electrolytes for Hybrid Battery/Supercapacitor Devices », *J. Electrochem. Soc.*, vol. 163, nº 14, p. A2956-A2964, janv. 2016, doi: 10.1149/2.0421614jes.